International Journal of Pharmaceutics 404 (2011) 231–237

Contents lists available at ScienceDirect

International Journal of Pharmaceutics

journal homepage: www.elsevier.com/locate/ijpharm

Pharmaceutical Nanotechnology

Preparation of a chemically stable quercetin formulation using nanosuspension technology

Lei Gao*, Guiyang Liu, Xiaoqing Wang, Fei Liu, Yuefang Xu, Jing Ma

Department of Pharmacy, The First Affiliated Hospital of General Hospital of PLA, No. 51 Fucheng Road, Beijing 100048, China

ARTICLE INFO

Article history:
Received 13 March 2010
Received in revised form 27 October 2010
Accepted 10 November 2010
Available online 17 November 2010

Keywords:
Quercetin
Stability
Poorly soluble drugs
High pressure homogenization
Precipitation
Crystalline state

ABSTRACT

In the present study the evaporative precipitation into aqueous solution (EPAS) process and the high homogenization press (HPH) process were compared to evaluate their feasibility to form a chemically stable quercetin nanosuspension. The particle size and Zeta potential of the EPAS nanosuspension were similar to those of the HPH nanosuspension. Differences in results of differential scanning calorimetery and X-ray measures were observed between the two processes. The crystalline-to-amorphous phase transition was shown in the profile of EPAS dried powder. On the contrary the initial crystalline state of drug was maintained throughout the HPH process. Dissolution test results indicated that the EPAS process showed a higher improvement in the drug solubility and dissolution rate than the HPH process. At last the High performance liquid chromatography (HPLC) analysis proved the superiority of both nanosuspensions over QCT solution formulation for the chemical and photo-stability. As a result, it can be concluded that the EPAS and HPH techniques were feasible to prepare a chemically stable QCT nanosuspension with significantly enhanced dissolution rate.

© 2010 Elsevier B.V. All rights reserved.

1. Introduction

Quercetin (QCT, 3,3′,4′,5,7-pentahydroxyflavone, Fig. 1) is a kind of natural flavonoids, which has been shown to have a variety of biological activities and pharmacological actions, such as dilating coronary arteries, decreasing blood lipid, anti-inflammation, anti-oxidation and anti-tumor activities (Hollman and Kata, 1999; Lugli et al., 2009). However, QCT present a very low bioavailability (less than 17% in rats and even 1% in human), which results in that the biological effects of QCT as determined in *in vitro* assays cannot be directly transferred to *in vivo* conditions (Chan et al., 2003; Khaled et al., 2003). Apart from the considerable metabolism and high plasma protein binding *in vivo* (99.4%), its poor solubility (ca. 10 mg/L in water at ambient temperature) leading to very limited and slow absorption is also an important factor limiting the bioavailability (Bhattaram et al., 2002). Due to the low solubility, solution formulation of QCT for intravenous application is more challenging when a high bioavailability and a rapid onset of action are required. In addition, due to its parent skeleton of flavonoids, QCT is chemo- and thermolabile and rapidly degraded and discolored when exposed to alkaline media, photo and warm temperature (Scalia and Mezzena, 2009; Calabrò et al., 2004). Therefore the QCT solution formulation containing solubilizer or cosolvent (e.g. ethanol, Cremophor EL, etc) may experience degradation during the production and storage progress.

Recently, the nanosuspension technology has been successfully applied to tackle the formulation issue of the poorly soluble drugs. Nanosuspension is a carrier-free colloid drug delivery system containing only minimum stabilizers and pure drug particles with a mean particle size in the nanometer range, typically between 10 and 1000 nm (Keck and Müller, 2006; Gao et al., 2008). Outstanding nanosuspension properties such as increased drug solubility, high dispersity and homogenization, intravenously injectable, simple production process, universal adaptivity enable its applications in the formulation of large amounts of poorly soluble compounds. Furthermore, the formation of suspensions is one of effective approaches for the stabilization of chemically labile molecules insoluble in aqueous solution (Schwitzera et al., 2004; Pu et al., 2009).

Generally, the nanosuspension techniques are classified as bottom up processes and top down processes according to the differences of the production principle (Keck and Müller, 2006). In the bottom up processes the poorly water-soluble drug is first dissolved in an organic solvent and then precipitated through a non-solvent addition in the present of stabilizers, as in supercritical fluid (SCF) technology, evaporative precipitation into aqueous solution (EPAS), spray-freezing into liquid process, and emulsion-solvent evaporation (Li et al., 2007; Rabinow, 2004). These processes were simple and cost effective without any high energy input. However the following prerequisites should be met: (i) the drug should be soluble at least in one solvent. (ii) The solvent is miscible with a non-solvent

* Corresponding author. Tel.: +86 10 66867007; fax: +86 10 66867007.
E-mail address: business_gaolei@yahoo.cn (L. Gao).

0378-5173/$ – see front matter © 2010 Elsevier B.V. All rights reserved.
doi:10.1016/j.ijpharm.2010.11.009

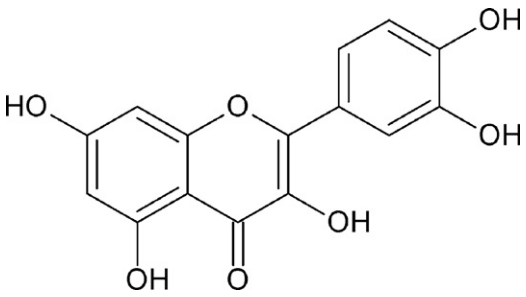

Fig. 1. Chemical structure of the quercetin (3,3′,4′,5,7-pentahydroxyflavone).

(Gao et al., 2008). The top down methods means the mechanical comminution processes of larger drug particles, as in media milling, microfluidization and high press homogenization (HPH) (Van Eerdenbrugh et al., 2008). These methods require no harsh solvents but involve high energy input and low power efficiency (Patravale et al., 2004; Liversidge et al., 2003). In addition some measures should be taken to minimize the degradation of heat sensitive drugs resulted from the heat generated in the comminution progress (Gao et al., 2008).

The aim of this study was to compare the EPAS process (bottom-up) and the HPH process (top-down) for the preparation of QCT nanosuspension. QCT nanosuspension was characterized in terms of particle size, size distribution, thermal properties and X-ray powder diffraction. The solubility and dissolution behavior of QCT before and following EPAS and HPH process were also compared. At last the chemico- and photo-stability of nanosuspension were evaluated over the monitoring period.

2. Materials and methods

2.1. Materials

QCT (95.0%) was purchased from Zelang herbs Company (Nanjing, China). QCT standard (98.0%) was purchased from the Shanhai Tongtian Co. Ltd. Pluronic F68 and lecithin was purchased from the Sigma-Aldrich Chemical Co. (USA). Acetonitrile used was of HPLC grade, and other materials were of analytical grade.

2.2. HPLC analysis

HPLC analysis of QCT was performed on an Agilent 1200 series HPLC system (Agilent, USA) equipped with an autosampler system and a variable wavelength UV detector. The detection wavelength was set at 373 nm. Chromatographic separation was carried out with a Eclipse XDB-C_{18} column (150 mm × 4.6 mm, 5 μm; Agilent, USA) with mobile phase of acetonitrile/5% acetic acid solution (27:73, v/v) at 30 °C. The flow rate was 1.0 mL/min. The QCT suspension samples were detected by HPLC following solution and dilution in q.s. methanol.

The calibration curve was linear within the range of 0.1–200 μg/mL ($y = 360.44x - 9.7499$, $r = 0.9998$). The detection limit (signal to noise ratio of 3:1) and quantification limit (signal to noise ratio of 10:1) were 0.02 μg/mL and 0.07 μg/mL, respectively. Within-day precision was determined by injecting five standard solutions of three different concentrations on the same day ($n = 5$) and between-day precision was determined by injecting the same solutions for consecutive five days. The relative standard deviation (RSD %) ranged between 0.49% and 1.48%. The accuracy of the method was performed by the standard addition technique. Three levels of solutions were made and injected, the recovery% ranged from 98.72% to 101.50% and RSD% ranged between 0.36% and 1.32%.

2.3. Nanosizing processes

2.3.1. EPAS process

0.2 g of QCT was dissolved in 5 mL of ethanol (60 °C) as an organic phase. The organic phase was added dropwise into 20 mL of solution containing Pluronic F68 (0.75%, w/v) and lecithin (0.25%, w/v) at 0 °C under continuous stirring at 2000 rpm with a propeller mixer (IKA, RW20, Germany). Then stirring at 300 rpm was maintained for 2 h at room temperature under vacuum at −25 in. Hg in order to decrease the ethanol content to a very low residual level, and then the EPAS nanosuspension was obtained (Pignatello et al., 2006).

2.3.2. HPH process

Pluronic F68 (0.75%, w/v) and lecithin (0.25%, w/v) were completely dispersed in 20 mL water. Then the QCT powder (1%, w/v) was dispersed into the solution and processed using a Fluko homogenizer (Shanghai, China) at 10000 rpm for 1 min, the resultant suspension was then circulated for two cycles at 200 bar pressure and five cycles at 500 bar, followed by another 20 cycles at 1500 bar using a piston-gap high pressure homogenizer (ATS HD100, Canada) to obtain the HPH nanosuspension. A circulating cold water/ethanol bath system (SDC-6, Ningbo Sicentz Biotechnology Co., Ltd., China) was utilized during the HPH process.

2.4. Water removal

First the QCT nanoparticles were gathered from nanosuspension by centrifugation using an ultracentrifuge (Biofuge stratos, Kendro Laboratory Products, Osterode, Germany) at 4 °C and rotate speed of 20,000 rpm for 30 min. Then the upper clear liquid was removed and the remaining residue was dried in a heated vacuum desiccator at 40 °C and −25 in. Hg (Ali et al., 2009).

2.5. Characterization of nanosuspension

2.5.1. Particle size, morphology and Zeta potential of QCT nanosuspension

The particle size and Zeta potential of QCT nanosuspension were measured with a Zetasizer (3000SH, Malvern Instruments Ltd., UK). All measurements were made in triplicate and the mean values and standard deviations were reported. The morphology of nanosuspensions was observed using TEM (JEM-1200EX, Japan). One drop of nanosuspensions was placed on a copper grid and stained with 2% phosphotungstic acid solution for 2 min. The grid was allowed to dry at room temperature and was examined with the electron microscope. To investigate whether the particle size and morphology changed before and after the water removal, the TEM and particle size distribution tests were also performed for the dried powder following re-dispersion in the QCT-saturated water.

2.5.2. Differential scanning calorimetery (DSC) analysis

Thermal properties of the powder samples were investigated with a differential scanning calorimeter (CDR-4P, Shanghai, China). Approximate 10 mg of sample was analyzed in an open aluminium pan, and heated at scanning rate of 10 °C/min between 0 °C and 400 °C. Magnesia was used as the standard reference material to calibrate the temperature and energy scale of the DSC apparatus. To evaluate the internal structure modifications of the drugs before and after nanosizing process, thermal analysis was performed on QCT, Pluronic F68, lecithin, their physical mixtures and the freeze-dried suspension powder.

2.5.3. X-ray powder diffraction (XRPD) measurements

The crystalline state of the samples was estimated by an X-ray diffractometer (D/max r-B, Rigaku, Japan). The experiments were performed in symmetrical reflection mode with a Cu line as the

Table 1
The comparison for characteristics of nanosuspension by EPAS process and HPH process, results were described as means ± S.D. ($n = 3$).

	EPAS nanosuspension		HPH nanosuspension	
	Before water removal	After water removal	Before water removal	After water removal
Particle size (nm)	251.6 ± 24.6	282.6 ± 50.3	192.47 ± 31.8	213.6 ± 29.3
Polydispersity index	0.23 ± 0.08	0.29 ± 0.02	0.21 ± 0.10	0.24 ± 0.08
Zeta potential (mV)	−23.23 ± 1.3	−21.12 ± 2.7	−22.57 ± 1.2	−22.48 ± 4.6

source of radiation. Standard runs using a 40 kV voltage, a 40 mA current and a scanning rate of 0.02° min^{-1} over a 2θ range of 5–40° were used. The samples analyzed were the same as the DSC experiments.

2.5.4. Drug solubility

To compare the solubility of the QCT before and following nanosizing process, saturation solubility was determined using a constant-temperature shaker (THX-82, Shanghai, China). Samples containing equivalent QCT (20 mg) were dispersed into 20 mL phosphate buffered solution (PBS, pH 6.8), the temperature and shake rate were set at 37 °C and 100 min^{-1}, respectively. After 48 h 3 mL of medium was withdrawn and placed in Ultrafree tube with a cutoff of 10,000 Da (Ultrafree, MC Millipore, Bedford, USA) and centrifuged at 20,000 × *g* for 30 min at 4 °C (Biofuge stratos, Kendro Laboratory Products, Osterode, Germany). The QCT content was measured by using the HPLC mentioned in Section 2.2. The experiments were made in triplicate.

2.5.5. Dissolution

Dissolution behavior of the QCT *in vitro* was estimated using a dissolution apparatus (RC-3B, Tianjin, China) with the paddle method. Samples containing equivalent of QCT (10 mg) were dispersed into 900 mL PBS (6.8) (containing 5% ethanol) after being pre- homogenized in ca. 5 mL dissolution medium. The temperature and rate were set at 37 °C and 100 min^{-1}, respectively. At predetermined intervals, 1 mL of medium was withdrawn and placed in Ultrafree tube with a cutoff of 10,000 Da (Ultrafree, MC Millipore, Bedford, USA) and centrifuged at 20,000 × *g* for 30 min at 4 °C (Biofuge stratos, Kendro Laboratory Products, Osterode, Germany). Equal blank medium was compensated immediately to sustain the sink condition following each sampling. The QCT content was measured by using the HPLC mentioned in Section 2.2. Each sample was analyzed in triplicate.

2.6. Chemical and photo-stability

For the chemical stability studies, all samples were kept in siliconized glass vials at 25 °C (no light) for 1 month; to evaluate the photo-stability of the QCT, all samples was exposed to a continuous illuminance of 2500 Lx supplied by a fluorescent lamps for 10 days. At predetermined time intervals, approximate 10 μL aliquot of samples was drawn out for further analysis. The drug content of QCT was tested by using HPLC method mentioned in Section 2.2. All samples were analyzed in triplicate.

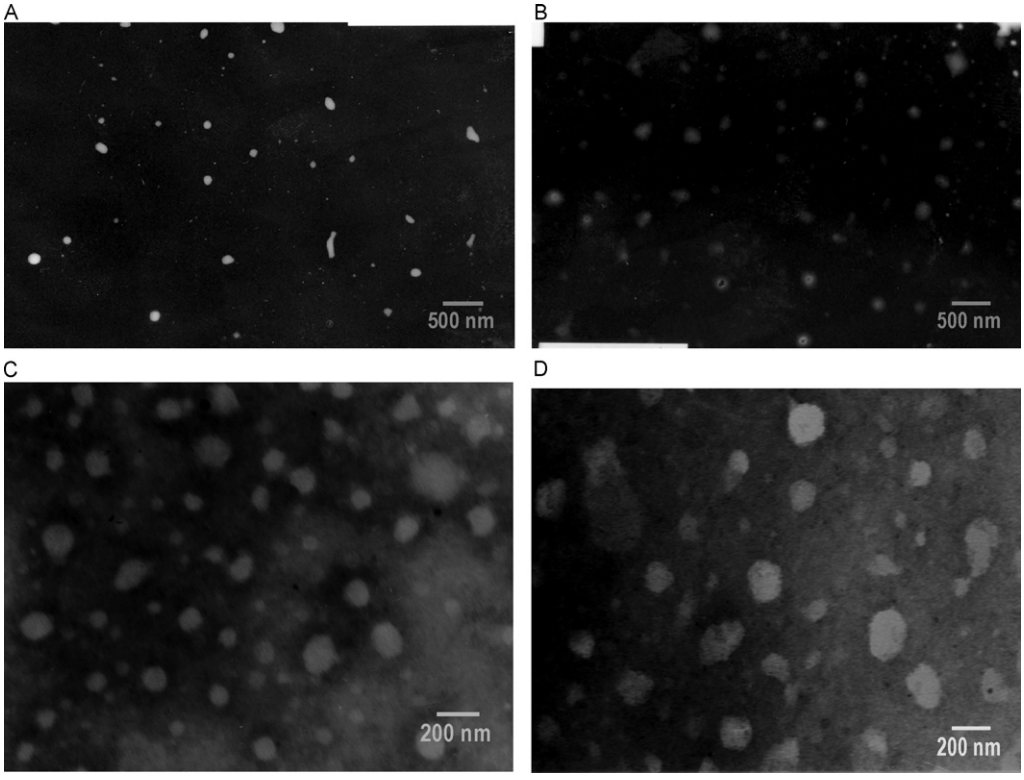

Fig. 2. TEM photographs of EPAS nanosuspension and HPH nanosuspension before and after water removal: (A) EPAS nanosuspension before water removal (20,000×); (B) EPAS nanosuspension after water removal (20,000×); (C) HPH nanosuspension before water removal (40,000×); (D) HPH nanosuspension after water removal (40,000×).

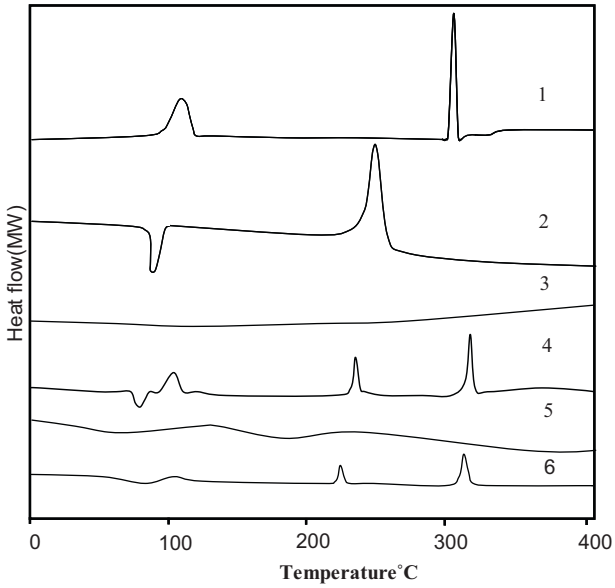

Fig. 3. Differential scanning calorimetry thermograms for: (1) QCT; (2) Pluronic F68; (3) lecithin; (4) physical mixture of QCT, Pluronic F68 and lecithin; (5) EPAS dried powder; (6) HPH dried powder.

3. Results

3.1. Particle size, morphology and Zeta potential of QCT nanosuspension

The particle size and Zeta potential of EPAS nanosuspension and HPH nanosuspension were shown in Table 1. The mean particle size of EPAS suspension was 251.56 ± 24.6 nm with a polydispersity index of 0.23 ± 0.08, and the mean particle size of HPH suspensions was 192.47 ± 31.8 nm with a polydispersity index of 0.21 ± 0.10. TEM photos (Fig. 2) showed that after nanosization, both EPAS and HPH, the large crystals were transformed into round or cubic nanoparticles. It could be found that the particle size and Zeta potential of the nanosuspensions exhibited no essential changes before and after the water removal. Following re-dispersion of the dried powders, the mean paricle size of the EPAS and HPH nanosuspension were 282.6 ± 50.3 nm and 213.6 ± 29.3 nm, respectively.

3.2. DSC analysis

Fig. 3 exhibited the DSC thermograms of the QCT, Pluronic F68, lecithin, physical mixture of QCT, Pluronic F68, lecithin, and QCT lyophilized powder from EPAS suspension and HPH suspension. The curve of the QCT showed two endothermic peaks: a broad endotherm between 80 °C and 120 °C corresponds to the loss of bounded water; the other was a sharp endothermic peak at 311 °C indicating the melting point. This result was consistent with others reports (Zheng and Chow, 2009; Borghetti et al., 2009). The Pluronic F68 showed a glass transition temperature at 79.6 °C followed by a melting point peak at 242.3 °C. No endothermic peak could be seen in the lecithin curve indicating the amorphous structure of the lecithin. In the thermogram of the physical mixture, there were peaks resulting from simple superposition of the DSC curves of the separate component in it. The powder dried from EPAS suspension and HPH suspension displayed DSC curves with substantial differences. There was no endothermic peak in the DSC curve of EPAS dried powder. However, the endothermic peaks of drug and excipients could be seen in the curve of HPH dried powder.

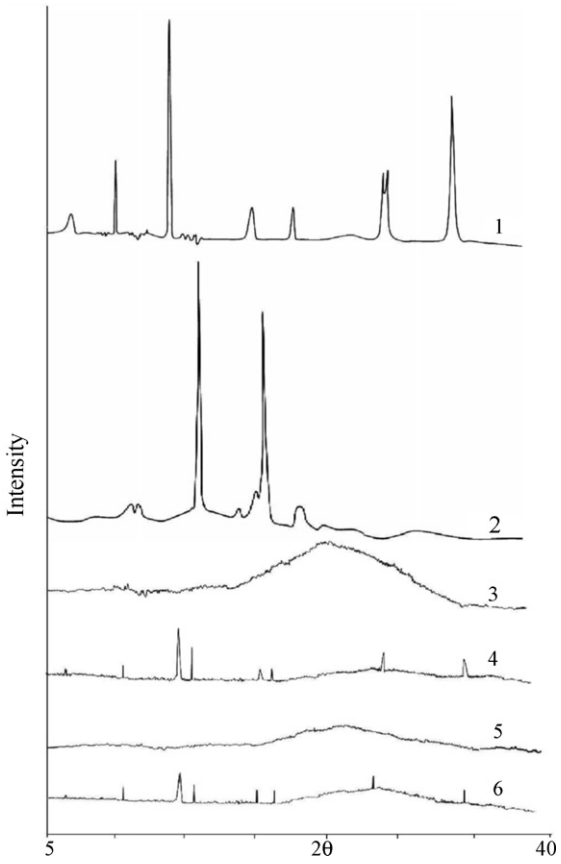

Fig. 4. XRPD diffractograms for: (1) QCT; (2) Pluronic F68; (3) lecithin; (4) physical mixture of QCT, Pluronic F68 and lecithin; (5) EPAS dried powder; (6) HPH dried powder.

3.3. XRPD analysis

The XRPD patterns of the QCT, Pluronic F68, lecithin, the physical mixture and lyophilized powder were as shown in Fig. 4. The XRPD of QCT exhibited intense peaks at 2θ of 8.2°, 14.0°, 28.6° and 33.6°, indicative of its crystalline nature. Pluronic F68 presented two intense peaks at 16.0° and 20.8°. A broad and diffuse pattern was apparent with lecithin, suggesting that it was essentially amorphous. The XRPD pattern of the physical mixture was a composite pattern of the individual compounds, indicating no formation of new physical state. The profile for EPAS dried powder was very flat with no intense peaks, indicating an essentially amorphous nature. However, the profile of HPH dried powder presented the characteristic peaks of QCT and Pluronic F68, indicative of the maintenance of the initial crystalline state.

3.4. Solubility and dissolution studies

The solubility of bulk QCT was only 10.28 μg/mL as shown in Fig. 5. The physical mixture showed a slightly increase in the solubility of QCT (16.42 μg/mL). A highest solubility was achieved for the EPAS dried powder, which was 422.4 μg/mL, much higher than that of the HPH dried powder, which was 278.6 μg/mL.

Fig. 6 showed the dissolution profiles of the four samples. Only 61.5% and 68.6% had dissolved at 24 h for the bulk QCT and the physical mixture, respectively. The dissolution rate of EPAS dried powder was so fast that 67.1% had dissolved at 10 min and 92.9% had dissolved within 20 min. The HPH powder dissolved 39.5% at 10 min and 73.2% at 20 min, slower than the EPAS powder.

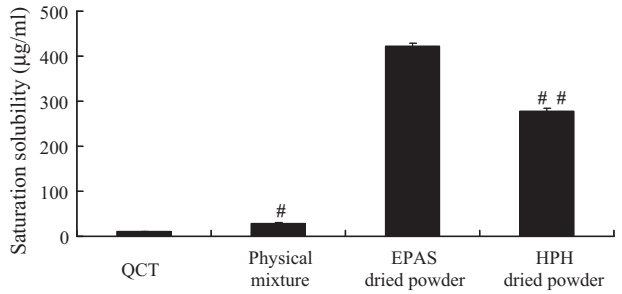

Fig. 5. Profiles of QCT solubility at 37 °C for bulk powder, physical mixture of QCT, Pluronic F68 and lecithin, EPAS dried powder and HPH dried powder. (# versus bulk QCT, $p < 0.05$; ## versus EPAS dried powder, $p < 0.01$).

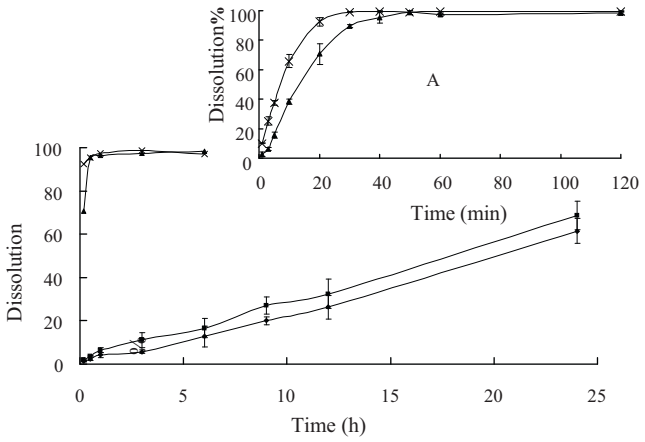

Fig. 6. Dissolution profiles for bulk QCT (-♦-), physical mixture of QCT, Pluronic F68 and lecithin (-■-) EPAS dried powder (-×-) and HPH dried powder (-▲-) at 37 °C and 100 rpm. (The inserted illustration A was the dissolution profile of the nanosuspensions within the first 2 h).

3.5. Chemical and photo-stability

The effects of nanosuspension technology on improving the chemical and photo-stability of QCT were investigated. Based on the maximum solubility of QCT in water (10.5 mg/L), a control water solution containing about 0.8 mg/100 mL was tested in parallel. Fig. 7 showed the degradation of QCT in different formulations over a 1 month period. Although stored at a temperate condition (at 25 °C/no light) a reduction of 28.3% in QCT content and obvious discoloration was observed for the solution over 1 month period. In contrast, both EPAS and HPH nanosuspension stored at the same conditions showed no significant alteration in drug content and in color over the monitoring period. Similar results were observed in the photostability studies, which showed that a reduction of 19.9% in drug content was found for the QCT solution but no significant reduction found for both nanosuspensions (Fig. 8).

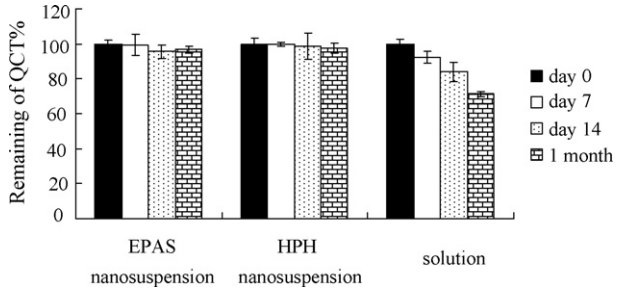

Fig. 7. Degradation of QCT in different formulations stored at 25 °C in the light-shielding condition.

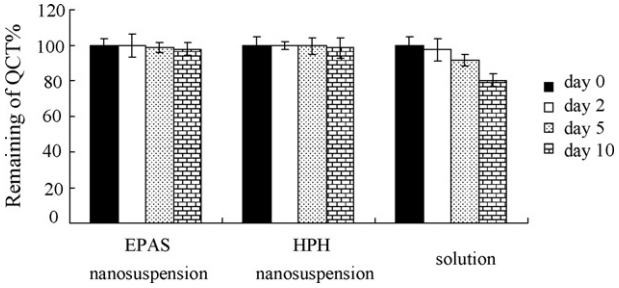

Fig. 8. Degradation of QCT in different formulations exposed to a continuous illuminance (2500 Lx supplied by a fluorescent lamps) for 10 days.

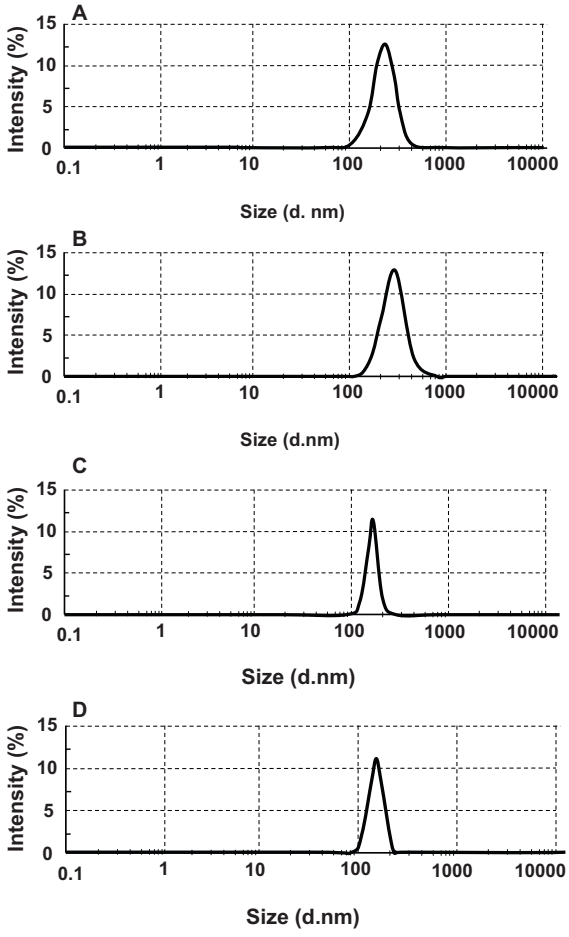

Fig. 9. Particle size distribution of EPAS nanosuspensionand HPH nanosuspension before and after water removal. (A) EPAS nanosuspension before water removal; (B) EPAS nanosuspension after water removal; (C) HPH nanosuspension before water removal; (D) HPH nanosuspension after water removal.

4. Discussions

From Fig. 9 and Table 1 we could see that the EPAS and HPH process both successfully leaded to the nanonization of the QCT with narrow size distribution, the mean particle size of EPAS suspension and HPH suspensions were 251.56 ± 24.6 nm and 192.47 ± 31.8 nm respectively. There was no statistical significant difference in Zeta potential between the two suspensions. The reason for this is that the Zeta potential of the nanosuspension was mainly dependent of the composition of the stabilizers (Ain-Ai and Gupta, 2008). It could be seen in Figs. 2 and 9 that particle size and morphology for both nanosuspensions showed no changes essentially before

and after water removal. In the progress of the nanosization, it was the hydrophobic/hydrophilic interactions of surfactant molecules and drug for firm anchoring on the newly generated particle surface (Müller and Jacobs, 2002). Therefore, most of the stabilizers would keep anchoring on the surface of the particles and precipitate together with the nanoparticles after high centrifugalization. With the effects of the coverage layer of stabilizers the dried powder could be finely re-dispersed in the water.

Both nanosuspensions show a good physical stability with a moderate size increase during 1 month of monitoring (data not shown), however, further investigation of physical stability was not performed, because the long-term physical stability was not the aim of the present studies, it would be investigated in detail in the future research.

The alteration of the physical state of the substances before and after the formation could be analyzed through DSC and XRPD studies. DSC was performed to investigate the interaction between the drugs and the excipients during the fabrication process and evaluate the effect of the excipients on the inner structure of drugs. XRPD could be used to analyze potential changes in the inner structure of drug crystals during the nanosizing process. Fig. 3 showed that there were peaks resulting from simple superposition of the DSC curves of the separate component in the thermogram of the physical mixture. It was interesting that the powder dried from EPAS suspension and HPH suspension displayed DSC curves with substantial differences: no endothermic peak presented in the DSC curve of EPAS dried powder; in the contrast, the endothermic peaks of drug and excipients could be seen in the curve of HPH dried powder. Similar results could be obtained in the XRPD profiles, which also indicated an essentially amorphous nature for EPAS dried powder and the maintenance of the initial crystalline state for the HPH dried powder (Fig. 4). These differences indicated that the EPAS process and HPH process had opposite effects on the physical state of the drug.

The differences between EPAS dried powder and HPH dried powder in physical state might result from the different production principles. The HPH process mechanically breaks the microparticles preferentially at weak points, i.e. imperfections. With the process of the comminution the number of imperfections is getting less and less and the crystals remaining are becoming more and more perfect. When the mechanical force is equal to the interaction forces in the crystal, the particles will not further diminute, and the drug retains the original crystalline structure (Keck and Müller, 2006). However, the EPAS process involves the reconstruction of drug molecules liberated from the original crystals in the anti-solvent. In this process the coexisted surfactant molecules might inhibit the growth of drug crystals as their interaction prevents the packing of drug molecules in their preferable orientation and hence amorphous phase forms (Hancock and Parks, 2000). In addition, the rapid evaporation of the organic solvent in EPAS process with the proximity of the aqueous stabilizer to the nascent drug particles may result in fast nucleation leading to amorphous nanoparticles (Sarkari et al., 2002). These findings about the crystalline state of nanoparticles from EPAS and HPH process were in line with the reports for some other compounds. It was found that the EPAS process leaded to a crystalline-to-amorphous transition for hydrocortisone (Ali et al., 2009), carbamazepine (Sarkari et al., 2002) and cyclosporine A (Chen et al., 2002). However, the crystalline nature were maintained throughout the HPH process for nifedipine (Hecq et al., 2005), ucb-35440–3 (Hecq et al., 2006) and oridonin (Gao et al., 2007).

Fig. 5 showed that the two nano-sized powders exhibited approximate 41-fold and 27-fold increase in the solubility respectively compared to the bulk QCT. The reason for the sharp increase is that the saturation solubility is a function of particle size when the particle size is reduced to the nanometer range according to the Ostwald–Freundlich equation (Böhm and Müller, 1999):

$$\log \frac{C_s}{C_\infty} = \frac{2\nu\sigma}{2.303RT\rho\gamma} \quad (1)$$

where C_s is the solubility, C_∞ is the solubility of the solid consisting of large particles, σ is the interfacial tension, ν is the molar volume of the particle material, R is the gas constant, T is absolute temperature, ρ is the density of the solid, and r is the radius of particles material.

Considering the same formulation composition and similar particle size, the higher solubility of the EPAS dried powder compared to the HPH dried powder could be ascribed to its amorphous state. It was well known that the amorphous state characterized by higher energy showed relative higher solubility compared with the crystalline state (Hancock et al., 2002).

Besides the increase in saturation solubility, enhancement of the dissolution rate was also achieved for the nano-sized powder as shown in Fig. 6. From the Noyes–Whitney equation (Hintz and Johnson, 1989), we knew that the increased surface area and saturation solubility resulting from the particle radius in nanometer range led to the increased dissolution velocity. The difference in dissolution rate between the EPAS dried powder and HPH dried powder was also contributed to the substantial difference in the physical state. Similar results were reported by Sarkari et al. (2002), who found that the less crystalline powder showed the higher dissolution rate.

Results of the stability studies proved that nanosuspension could significantly improve the chemical- and photo-stability of QCT compared with the solution stored in the same conditions (Figs. 7 and 8). This finding could be explained by two effects. First the molecules of the stabilizers covering on the surface of the nanoparticles could shield the inner compound (Schwitzera et al., 2004). Second, for the nanosuspension only the particle surface is accessible to water and light, that means there will be the formation of a degraded outer monolayer of molecules protecting the inner part of the drug nanoparticles (similar to oxidized layer on top of aluminium) (Müller and Keck, 2004). In addition, due to the protection of the stabilizer layer, even in this outer layer only a few molecules will be degraded. It could be concluded from these findings that nanosuspension technology would be an effective route to improve the stabilization of the chemical labile drugs.

5. Conclusion

Both EPAS and HPH process were shown to be a simple and adequate operation to fabricate QCT nanosuspension. The two processes exhibited opposite effects on the physical state throughout the production, crystalline state of QCT was shown not to be altered through HPH process, and a crystalline-to-amorphous phase transition occurred through EPAS process. The EPAS nanosuspension showed higher improvement in drug solubility and dissolution rate compared to the HPH suspension due to its higher inner energy related to the amorphous phase. Remarkable improvement in chemical and photo-stability of QCT molecules in nanosuspension was observed compared with the solution. The increased chemical stability could not only hold the activity but also reduce the toxicity of QCT. The present studies demonstrated that both the EPAS and HPH process could be utilized as a useful method for preparing a chemically stable QCT nanosuspension.

Acknowledgements

Institute of Radiation Medicine, Academy of Military Medical Science, Beijng, China is gratefully acknowledged for supporting the Zetasizer machine. We are grateful for editorial assistance provide by Dr. Luan.

References

Ain-Ai, A., Gupta, P.K., 2008. Effect of arginine hydrochloride and hydroxypropyl cellulose as stabilizers on the physical stability of high drug loading nanosuspension of a poorly soluble compound. Int. J. Pharm. 351, 282–288.

Ali, H.S.M., York, P., Blagden, N., 2009. Preparation of hydrocortisone nanosuspension through a bottom-up nanoprecipitation technique using microfluidic reactors. Int. J. Pharm. 375, 107–113.

Bhattaram, V.A., Graefe, U., Kohlert, C., Veit, M., Derendorf, H., 2002. Pharmacokinetics and bioavailability of herbal medicinal products. Phytomedicine 9, 1–33.

Böhm, B.H.L., Müller, R.H., 1999. Lab-scale production unit design for nanosuspension of sparingly soluble cytotoxic drugs. Pharm. Sci. Technol. Today 2, 336–339.

Borghetti, G.S., Lula, I.S., Sinisterra, R.D., Bassani, V.L., 2009. Quercetin/β-cyclodextrin solid complexes prepared in aqueous solution followed by spray-drying or by physical mixture. AAPS Pharm. Sci. Technol. 10, 235–242.

Calabrò, M.L., Tommasini, S., Donato, P., Raneri, D., Stancanelli, R., Ficarra, P., Ficarra, R., Costa, C., Catania, S., Rustichelli, C., Gamberini, G., 2004. Effects of α- and β-cyclodextrin complexation on the physico-chemical properties and antioxidant activity of some 3-hydroxyflavones. J. Pharm. Biomed. Anal. 35, 365–377.

Chan, M.M., Fong, D., Soprano, K.J., Holmes, W.F., Heverling, H., 2003. Inhibition of growth and sensitization to cisplatin-mediated killing of ovarian cancer cells by polyphenolic chemopreventive agents. J. Cell. Physiol. 194, 63–70.

Chen, X., Young, T.J., Sarkari, M., Williams III, R.O., Johnston, K.P., 2002. Preparation of cyclosporine A nanoparticles by evaporative precipitation into aqueous solution. Int. J. Pharm. 242, 3–14.

Gao, L., Zhang, D., Chen, M., Zheng, T., Wang, S., 2007. Preparation and characterization of an oridonin nanosuspension for solubility and dissolution velocity enhancement. Drug Dev. Ind. Pharm. 33, 1332–1339.

Gao, L., Zhang, D., Chen, M., 2008. Drug nanocrystals for the formulation of poorly soluble drugs and its application as a potential drug delivery system. J. Nanopart. Res. 10, 845–862.

Hancock, B., Parks, M., 2000. What is the true solubility advantage for amorphous pharmaceuticals. Pharm. Res. 17, 397–404.

Hancock, B.C., Carlson, G.T., Ladipo, D.D., Langdon, B.A., Mullarney, M.P., 2002. Comparison of the mechanical properties of the crystalline and amorphous forms of a drug substance. Int. J. Pharm. 241, 73–85.

Hecq, J., Deleers, M., Fanara, D., Vranckx, H., Amighi, K., 2005. Preparation and characterization of nanocrystals for solubility and dissolution rate enhancement of nifedipine. Int. J. Pharm. 299, 167–177.

Hecq, J., Deleers, M., Fanara, D., Vranckx, H., Boulanger, P., Lamer, S.L., Amighi, K., 2006. Preparation and *in vitro*/*in vivo* evaluation of nano-sized crystals for dissolution rate enhancement of ucb-35440-3, a highly dosed poorly water-soluble weak base. Eur. J. Pharm. Biopharm. 64, 360–368.

Hintz, R.J., Johnson, K.C., 1989. The effect of particle size distribution on dissolution rate and oral absorption. Int. J. Pharm. 51, 9–17.

Hollman, P.C., Kata, M.B., 1999. Dietary flavonoids: intake, health effects and bioavailability. Food Chem. Toxicol. 37, 937–942.

Keck, C.M., Müller, R.H., 2006. Drug nanocrystals of poorly soluble drugs produced by high pressure homogenization. Eur. Pharm. Biopharm. 62, 3–16.

Khaled, K.A., El-Sayed, Y.M., Al-Hadiya, B.M., 2003. Disposition of the flavonoid quercetin in rats after single intravenous and oral doses. Drug Dev. Ind. Pharm. 29, 397–403.

Li, X.S., Wang, J.X., Shen, Z.G., Zhang, P.Y., Chen, J.F., Yun, J., 2007. Preparation of uniform prednisolone microcrystals by a controlled microprecipitation method. Int. J. Pharm. 342, 26–32.

Liversidge, E.M., Liversidge, G.G., Cooper, E.R., 2003. Nanosizing: a formulation approach for poorly-water-soluble compounds. Eur. J. Pharm. Sci. 18, 113–120.

Lugli, E., Ferraresi, R., Roat, E., Troiano, L., Pinti, M., Nasi, M., Neme, E., Bertoncelli, L., Gibellini, L., Salomoni, P., Cooper, E.L., Cossarizza, A., 2009. Quercetin inhibits lymphocyte activation and proliferation without inducing apoptosis in peripheral mononuclear cells. Leuk. Res. 33, 140–150.

Müller, R.H., Jacobs, C., 2002. Buparvaquone mucoadhesive nanosuspension: preparation, optimization and long-term stability. Int. J. Pharm. 237, 151–161.

Müller, R.H., Keck, C.M., 2004. Challenges and solutions for the delivery of biotech drugs–a review of drug nanocrystal technology and lipid nanoparticles. J. Biotechnol. 113, 151–170.

Patravale, V.B., Date, A.A., Kulkarni, R.M., 2004. Nanosuspension: a promsing drug delivery strategy. J. Pharm. Pharmacol. 56, 827–840.

Pignatello, R., Ricupero, N., Bucolo, C., Maugeri, F., Maltese, A., Puglisi, G., 2006. Preparation and characterization of eudragit retard nanosuspensions for the ocular delivery of cloricromene. AAPS Pharm. Sci. Technol. 7, E27.

Pu, X., Sun, J., Wang, Y., Wang, Y., Liu, X., Zhang, P., Tang, X., Pan, W., Han, J., He, Z., 2009. Development of a chemically stable 10-hydroxycamptothecin nanosuspension. Int. J. Pharm. 379, 167–173.

Rabinow, B.E., 2004. Nanosuspension in drug delivery. Nat. Rev. Drug Discov. 3, 785–796.

Sarkari, M., Brown, J., Chen, X., Swinnea, S., Williams III, R.O., Johnston, K.P., 2002. Enhanced drug dissolution using evaporative precipitation into aqueous solution. Int. J. Pharm. 243, 17–31.

Scalia, S., Mezzena, M., 2009. Incorporation of quercetin in lipid microparticles: effect on photo- and chemical-stability. J. Pharm. Biomed. Anal. 49, 90–94.

Schwitzera, J.M., Achleitner, G., Pomperb, H., Müller, R.H., 2004. Development of an intravenously injectable chemically stable aqueous omeprazole formulation using nanosuspension technology. Eur. Pharm. Biopharm. 58, 615–619.

Van Eerdenbrugh, B., Van den Mooter, G., Augustijns, P., 2008. Top-down production of drug nanocrystals: nanosuspension stabilization, miniaturization and transformation into solid products. Int. J. Pharm. 364, 64–75.

Zheng, Y., Chow, A.H.L., 2009. Production and characterization of a spray-dried hydroxypropyl-β-cyclodextrin/quercetin complex. Drug Dev. Ind. Pharm. 35, 727–734.